Continuous-variable quantum teleportation with non-Gaussian resources

F. Dell'Anno,[1,2,3] S. De Siena,[2,3] L. Albano,[1,3] and F. Illuminati[1,3,4,*]

[1]*Dipartimento di Matematica e Informatica, Università degli Studi di Salerno, Via Ponte don Melillo, I-84084 Fisciano (SA), Italy*

[2]*Dipartimento di Fisica, Università degli Studi di Salerno, Via S. Allende, I-84081 Baronissi (SA), Italy*

[3]*CNR-INFM Coherentia, Napoli, Italy and CNISM Unità di Salerno and INFN Sezione di Napoli, Gruppo Collegato di Salerno, Baronissi (SA), Italy*

[4]*ISI Foundation for Scientific Interchange, Viale Settimio Severo 65, 00173 Torino, Italy*

(Received 26 June 2007; published 2 August 2007)

We investigate continuous variable quantum teleportation using non-Gaussian states of the radiation field as entangled resources. We compare the performance of different classes of degaussified resources, including two-mode photon-added and two-mode photon-subtracted squeezed states. We then introduce a class of two-mode squeezed Bell-like states with one-parameter dependence for optimization. These states interpolate between and include as subcases different classes of degaussified resources. We show that optimized squeezed Bell-like resources yield a remarkable improvement in the fidelity of teleportation both for coherent and nonclassical input states. The investigation reveals that the optimal non-Gaussian resources for continuous variable teleportation are those that most closely realize the simultaneous maximization of the content of entanglement, the degree of affinity with the two-mode squeezed vacuum, and the, suitably measured, amount of non-Gaussianity.

DOI: 10.1103/PhysRevA.76.022301 PACS number(s): 03.67.Hk, 03.67.Mn, 42.50.Dv, 42.65.Yj

I. INTRODUCTION

Recent theoretical and experimental effort in quantum optics and quantum information has been focused on the engineering of highly nonclassical, non-Gaussian states of the radiation field [1], in order to achieve either enhanced properties of entanglement or other desirable nonclassical features [1–5]. It has been shown that, at fixed covariance matrix, some of these properties, including entanglement and distillable secret key rate, are minimized by Gaussian states [6]. In the last two decades, increasingly sophisticated degaussification protocols have been proposed, based on photon addition or subtraction [7–11], and some of them have been recently experimentally implemented to engineer non-Gaussian photon-added and photon-subtracted states starting from Gaussian coherent or squeezed inputs [12–14].

Progress in the theoretical characterization and the experimental production of non-Gaussian states are being paralleled by the increasing attention on the role and uses of non-Gaussian entangled resources in quantum information and quantum computation with continuous-variable systems [15]. In particular, concerning quantum teleportation with continuous variables [16,17,20], it has been demonstrated that the fidelity of teleportation can be improved by exploiting suitable deguassifications of Gaussian resources [3,21–23]. Moreover, non-Gaussian cloning of coherent states has been shown to be optimal with respect to the single-clone fidelity [24]. Determining the performance of non-Gaussian entangled resources may prove useful in a number of concrete applications ranging from hybrid quantum computation [25] to cat-state logic [26] and, generically, in all quantum computation schemes based on communication that integrates together qubit degrees of freedom for computation with quantum continuous variables for communication and interaction [27].

In the present work, we investigate systematically the performance of different classes of entangled two-mode non-Gaussian states used as resources for continuous-variable quantum teleportation. In our approach, the entangled resources are taken to be non-Gaussian *ab initio*, and their properties are characterized by the interplay between continuous-variable (CV) squeezing and discrete, single-photon pumping. Our first aim is to determine the actual properties of non-Gaussian resources that are needed to assure improved performance compared to the Gaussian case. At the same time, we carry out a comparative analysis between the different non-Gaussian cases in order to single out those properties that are most relevant to successful teleportation. Finally, we wish to understand the role of adjustable free parameters, in addition to squeezing, in order to "sculpture" and achieve optimized performances within the set of non-Gaussian resources. We will show that maximal non-Gaussian improvement of teleportation success depends on the nontrivial relations between enhanced entanglement, suitably measured level of *non-Gaussianity*, and the presence of a proper Gaussian squeezed-vacuum contribution in the non-Gaussian resources at large values of the squeezing (squeezed-vacuum affinity). We limit the discussion to general issues of principle, considering the ideal situation of pure-state resources in the absence of noise and imperfections. Detailed analysis of realistic situations with mixed-state resources in the presence of various sources of noise will be discussed elsewhere.

The paper is organized as follows. In Sec. II we introduce and describe relevant instances of two-mode entangled non-Gaussian resources, including squeezed number states and typical degaussified states currently considered in the literature, such as photon-added squeezed and photon-subtracted squeezed states. We show that all of the former, as well as the Gaussian two-mode vacuum and squeezed vacuum (twin

*Corresponding author. illuminati@sa.infn.it

beam), can be seen as particular subcases of a properly defined class of *squeezed Bell-like states* depending on a continuous angular parameter. In Sec. III, exploiting the unifying formalism of the characteristic function, we compare the relative performances of non-Gaussian and Gaussian resources in the Braunstein-Kimble CV teleportation protocol for different (single-mode) input states, Gaussian and non-Gaussian, including coherent and squeezed states, number states, photon-added coherent states, and squeezed number states. In Sec. IV we consider the optimization of non-Gaussian performance in CV teleportation with respect to the extra angular parameter of squeezed Bell-like states. We show that maximal teleportation fidelity is achieved by using a form of a squeezed Bell-like resource that differs both from squeezed number and photon-added or photon-subtracted squeezed states. In Sec. V we identify the properties that determine the maximization of the teleportation fidelity using non-Gaussian resources. We find that optimized non-Gaussian resources are those that come nearest to the simultaneous maximization of three distinct properties: The content of entanglement, the amount of (properly quantified) non-Gaussianity, and the degree of "vacuum affinity," i.e., the maximum, over all values of the squeezing parameter, of the overlap between a non-Gaussian resource and the Gaussian twin beam. Schemes for the experimental production of optimized squeezed Bell-like resources are illustrated in Sec. VI. Finally, in Sec. VII we present our conclusions and discuss some outlooks about the extension to other types of resources, optimized protocols, and applications to realistic situations in the presence of noise.

II. NON-GAUSSIAN RESOURCES: CHARACTERIZATION AND ENTANGLEMENT PROPERTIES

We begin our study by considering some different instances of two-mode entangled non-Gaussian states obtained by squeezing operations and mechanisms of photon addition or subtraction. Let us first introduce the following three classes of (normalized) pure states:

$$|\zeta;m_1,m_2\rangle = S_{12}(\zeta)|m_1,m_2\rangle_{12}, \tag{1}$$

$$|m_1^{(+)},m_2^{(+)};\zeta\rangle = \mathcal{N}_{12}^{(+)}a_1^{\dagger m_1}a_2^{\dagger m_2}S_{12}(\zeta)|0,0\rangle_{12}, \tag{2}$$

$$|m_1^{(-)},m_2^{(-)};\zeta\rangle = \mathcal{N}_{12}^{(-)}a_1^{m_1}a_2^{m_2}S_{12}(\zeta)|0,0\rangle_{12}, \tag{3}$$

where $S_{12}(\zeta)=e^{-\zeta a_1^\dagger a_2^\dagger+\zeta a_1 a_2}$ is the two-mode squeezing operator, $\zeta=re^{i\phi}$, $\mathcal{N}_{12}^{(\cdot)}$ are the normalizations, and $|m_1,m_2\rangle_{12} \equiv |m_1\rangle_1\otimes|m_2\rangle_2$ is a two-mode Fock state. Equations (1), (2) and (3) define the squeezed number states, the photon-added squeezed states, and the photon subtracted squeezed states, respectively. Letting $m_i^{(\cdot)}=0$, all states reduce to the Gaussian two-mode squeezed vacuum, i.e., the twin beam $|\zeta\rangle = S_{12}(\zeta)|0,0\rangle_{12}$. The normalization factors can be easily computed. For instance, if we take the explicit case $m_i^{(\cdot)}=1$, we have

$$|\zeta;1,1\rangle = S_{12}(\zeta)|1,1\rangle_{12}, \tag{4}$$

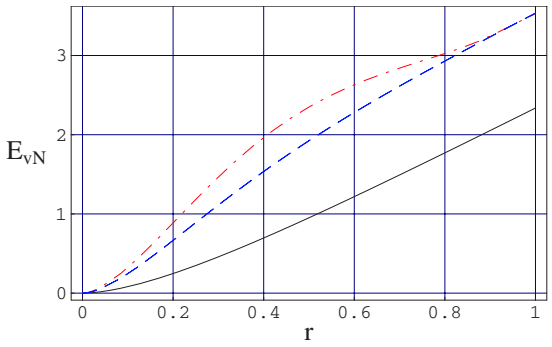

FIG. 1. (Color online) Behavior of the von Neumann entropy $E_{\rm vN}$ for the pure states (4)–(6) as a function of the modulus r of the squeezing parameter ζ. The upper curve (dotted-dashed line) corresponds to the squeezed number state $|\zeta;1,1\rangle$; the intermediate curve (dashed line) corresponds equivalently to the photon-added squeezed state $|1^{(+)},1^{(+)};\zeta\rangle$ and to the photon-subtracted squeezed state $|1^{(-)},1^{(-)};\zeta\rangle$. The lower curve corresponds to the twin beam $|\zeta\rangle$.

$$|1^{(+)},1^{(+)};\zeta\rangle = \mathcal{N}e^{-i\phi}S_{12}(\zeta)\{-\tanh r|0,0\rangle_{12}+e^{i\phi}|1,1\rangle_{12}\}, \tag{5}$$

$$|1^{(-)},1^{(-)};\zeta\rangle = \mathcal{N}e^{i\phi}S_{12}(\zeta)\{-|0,0\rangle_{12}+e^{i\phi}\tanh r|1,1\rangle_{12}\}, \tag{6}$$

where $\mathcal{N}=(1+\tanh^2 r)^{-1/2}$ is the normalization, and Eqs. (5) and (6) have been obtained by exploiting the two-mode Bogoliubov transformations

$$S_{12}^\dagger(\zeta)a_iS_{12}(\zeta) = \cosh r a_i - e^{i\phi}\sinh r a_j^\dagger (i\neq j=1,2)$$

We remark that both the photon-added and the photon-subtracted squeezed states are superpositions of the twin beam and of the squeezed number state. However, Eqs. (5) and (6) substantially differ for an exchange of the hyperbolic coefficients: In the limit of vanishing squeezing, the photon-added squeezed state reduces to a two-mode Fock state, remaining non-Gaussian, while the photon-subtracted squeezed state becomes Gaussian, as it reduces to the two-mode vacuum. In fact, all these states are particular instances of what we could name *squeezed Bell-like state*,

$$|\Psi\rangle_{\rm SB} = S_{12}(\zeta)\{\cos\delta|0,0\rangle_{12}+e^{i\theta}\sin\delta|1,1\rangle_{12}\}. \tag{7}$$

For instance, the squeezed number state (4) is recovered for $\delta=\pi/2$.

To quantify the bipartite entanglement of states (4)–(7) one needs the von Neumann entropy (entropy of entanglement) $E_{\rm vN}$. For the first three states, this quantity depends only on the modulus r of the squeezing parameter ζ. It is plotted in Fig. 1 and compared to that of the twin beam.

At a given squeezing, all the non-Gaussian states show an entanglement larger than that of the Gaussian squeezed vacuum. In particular, in the range of experimentally realistic values $0<r<1$ of the squeezing, the squeezed number state is the most entangled state. Moreover, the photon-added and the photon-subtracted squeezed states exhibit the same amount of entanglement at any r.

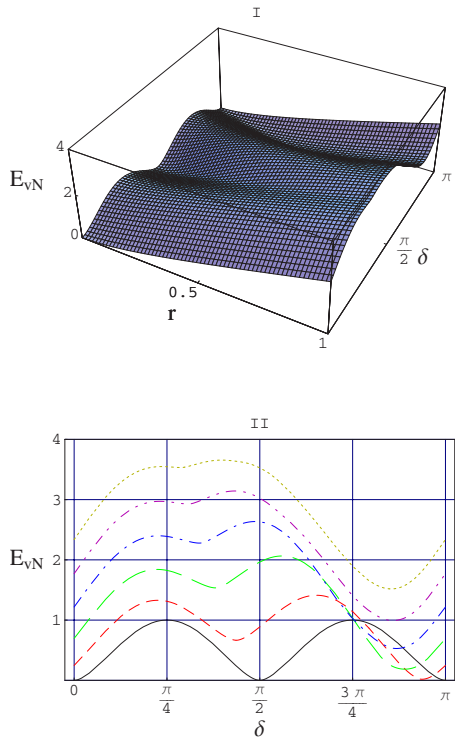

FIG. 2. (Color online) von Neumann entropy E_{vN} for the squeezed Bell-like state (7), as a function of r and δ. Panel I displays the three-dimensional plot of E_{vN}. Panel II displays two-dimensional projections at fixed squeezing strength r. Curves from bottom to top correspond to the different sections of E_{vN} as functions of δ for $r=0,0.2,0.4,0.6,0.8,1$.

The von Neumann entropy of the squeezed Bell-like state (7) is plotted in Fig. 2. In panel I we plot E_{vN} as a function of r and δ. In panel II, we can observe how the regular, oscillating behavior of the entropy for the Bell-like state ($r=0$) becomes gradually deformed by the optical pumping ($r\neq 0$), leading to a peculiar pattern of correlation properties for the squeezed Bell-like state (7).

III. TELEPORTATION IN THE CHARACTERISTIC FUNCTION REPRESENTATION

Quantum teleportation was first proposed by Bennett *et al.* in the discrete variable regime [28], and later experimentally demonstrated in that setting [29,30]. The idea of continuous-variable (CV) teleportation was put forward by Vaidman [31]. Some time later the actual quantum-optical protocol for the teleportation of quadrature amplitudes of a light field was introduced by Braunstein and Kimble in the formalism of the Wigner function [16], and realized by Furusawa *et al.* soon afterward [17–19]. In the standard CV protocol two users, Alice and Bob, share an entangled state (resource) of modes A and B; a single-mode input state $|\mathrm{in}\rangle$, in Alice's possession, is the state to be teleported. The protocol works as follows: The input mode "in" and mode A of the entangled resource are mixed at a 50:50 beam splitter, yielding the output modes in$'$ and A'. A destructive measurement (homodyne) is performed by Alice on the output modes in$'$ and A'. The obtained result is (classically) communicated to Bob; subsequently, Bob performs a unitary operation (displacement) on mode B, leading to the teleported state. For a comprehensive review on continuous-variable quantum teleportation and quantum information processing, see Ref. [20]. Various alternative descriptions of the original Braunstein-Kimble protocol have been introduced in the literature. Among them, we should mention those involving Fock state expansion [32], the coherent state expansion [33], and the transfer operator approach [34].

Recently, the CV teleportation protocol has been described in terms of the characteristic functions of the quantum states involved (input, resource, and teleported states) [35]. This formalism is particularly suited when dealing with non-Gaussian states and resources, because it greatly simplifies the calculational strategies. Let us denote by in$'$ and $\chi_{\mathrm{in}}(\alpha_{\mathrm{in}})$, respectively, the single-mode input state to be teleported and the associated characteristic function, and by ρ_{12} and $\chi_{12}(\alpha_1,\alpha_2)$, respectively, the entangled two-mode resource, shared by the sender and the receiver, and its characteristic function. By exploiting the Weyl expansion, it can be shown that the characteristic function $\chi_{\mathrm{out}}(\alpha_2)$ of the teleported state has the factorized form [35]

$$\chi_{\mathrm{out}}(\alpha_2)=\chi_{\mathrm{in}}(\alpha_2)\chi_{12}(\alpha_2^*,\alpha_2). \tag{8}$$

We should remark on the great simplicity, beauty, and power of this expression, particularly well suited in the study of teleportation-related subjects. In order to measure the success probability of a teleportation protocol, it is convenient to use the fidelity of teleportation $\mathcal{F}$. This is a state-dependent quantity that measures the overlap between the input state ρ_{in} and the output (teleported) state ρ_{out}, i.e., $\mathcal{F}=\mathrm{Tr}[\rho_{\mathrm{in}}\rho_{\mathrm{out}}]$. In the characteristic-function formalism, the fidelity reads

$$\mathcal{F}=\frac{1}{\pi}\int d^2\lambda\chi_{\mathrm{in}}(\lambda)\chi_{\mathrm{out}}(-\lambda). \tag{9}$$

In the following we will adopt Eq. (9) to analyze the efficiency of the CV teleportation protocol for different classes of input states and non-Gaussian entangled resources.

Let us first compute the symmetrically ordered characteristic function for the squeezed-number states, the photon-added, and the photon-subtracted squeezed states Eqs. (4)–(6). Being two-mode states, their characteristic function is of the form $\chi(\alpha_1,\alpha_2)=\mathrm{Tr}[D_1(\alpha_1)D_2(\alpha_2)\rho]$, where $D_i(\alpha_i)$ is the displacement operator corresponding to mode i, and ρ is the density operator associated to the state. We will make use of the relation

$$\langle m|D(\alpha)|n\rangle=\left(\frac{n!}{m!}\right)^{1/2}\alpha^{m-n}e^{-(1/2)|\alpha|^2}L_n^{(m-n)}(|\alpha|^2), \tag{10}$$

where $L_n^{(m-n)}(\cdot)$ is the associate Laguerre polynomial. The characteristic function for the state $|\zeta;1,1\rangle$ is

$$\chi_{SN}^{(1,1)}(\alpha_1,\alpha_2)=\chi_S(1-|\xi_1|^2)(1-|\xi_2|^2), \tag{11}$$

where

$$\chi_S(\alpha_1,\alpha_2) = e^{-(1/2)(|\xi_1|^2+|\xi_2|^2)} \tag{12}$$

is the characteristic function of the two-mode squeezed state, the standard reference Gaussian resource, and the implicit dependence on α_i stems from the relations

$$\xi_k = \alpha_k \cosh r + \alpha_l^* e^{i\phi} \sinh r \quad (k,l=1,2;k\neq l). \tag{13}$$

The characteristic functions for the states $|1^{(+)},1^{(+)};\zeta\rangle$ and $|1^{(-)},1^{(-)};\zeta\rangle$ read, respectively,

$$\chi_{PAS}^{(1,1)}(\alpha_1,\alpha_2) = \mathcal{N}^2\chi_S\{\tanh^2 r - 2\tanh r\,\mathrm{Re}[e^{-i\phi}\xi_1\xi_2] + (1-|\xi_1|^2)(1-|\xi_2|^2)\}, \tag{14}$$

$$\chi_{PSS}^{(1,1)}(\alpha_1,\alpha_2) = \mathcal{N}^2\chi_S\{1 - 2\tanh r\,\mathrm{Re}[e^{-i\phi}\xi_1\xi_2] + \tanh^2 r(1-|\xi_1|^2)(1-|\xi_2|^2)\}. \tag{15}$$

Comparing Eq. (12) with Eqs. (11), (14), and (15), we see that the polynomial non-Gaussian forms are always modulated by a Gaussian factor that coincides exactly with the squeezed-state characteristic function (12).

IV. TELEPORTATION WITH NON-GAUSSIAN RESOURCES

In this section we will compare the behavior of the fidelity for different input states by making use of the non-Gaussian entangled resources (4)–(6). The analysis will be carried out in terms of the entangling parameter ζ common to all resources. The following single-mode input states will be considered: Coherent states $|\beta\rangle$; squeezed states $|\varepsilon\rangle=S(\varepsilon)|0\rangle$, with $S(\varepsilon)=\exp\{-\frac{1}{2}\varepsilon a^{\dagger 2}+\frac{1}{2}\varepsilon^* a^2\}$ $(\varepsilon=e^{i\varphi}s)$; single-photon Fock states $|1\rangle$ photon-added coherent states $(1+|\beta|^2)^{-1/2}a^\dagger|\beta\rangle$; and squeezed single-photon Fock states $S(\varepsilon)|1\rangle$. The teleportation implemented with the two-mode squeezed Gaussian resource $|\zeta\rangle=S_{12}(\zeta)|0,0\rangle_{12}$ as entangled resource will be used as standard reference for comparison. Let us first consider the behavior of the fidelity for the Gaussian input states $|\beta\rangle$ and $|\varepsilon\rangle$, whose characteristic functions read

$$\chi_{\mathrm{coh}}(\alpha_{\mathrm{in}}) = e^{-(1/2)|\alpha_{\mathrm{in}}|^2+2i\,\mathrm{Im}[\alpha_{\mathrm{in}}\beta^*]}, \tag{16}$$

$$\chi_{\mathrm{sq}}(\alpha_{\mathrm{in}}) = e^{-(1/2)|\xi_{\mathrm{in}}|^2}, \tag{17}$$

where

$$\xi_{\mathrm{in}} = \alpha_{\mathrm{in}}\cosh s + \alpha_{\mathrm{in}}^* e^{i\varphi}\sinh s. \tag{18}$$

Let us remark that the fidelity is analytically computable for the classes of input states and entangled resources considered, as the integral in Eq. (9) can be exactly calculated in terms of finite sums of Gaussian averages.

In Fig. 3 we plot the fidelity $\mathcal{F}$ for input coherent states $|\beta\rangle$ (panel I), and input squeezed states (panel II).

We see that in both cases, the choice of the photon-subtracted squeezed state (6) as entangled resource is the most convenient one. It corresponds to the highest value of the fidelity $\mathcal{F}$ for any fixed value of the squeezing r (or, equivalently, of the energy) in the realistic range [0, 1]. On the contrary, the choice of the squeezed number state (4) as entangled resource is the least convenient, yielding the poorest performance even when compared to the Gaussian squeezed resource. Finally, regarding the use of the photon-added squeezed state (5) as entangled resource, it allows for a very modest improvement in the fidelity compared to the Gaussian resource, and this is only for a small interval of values around $r=1$.

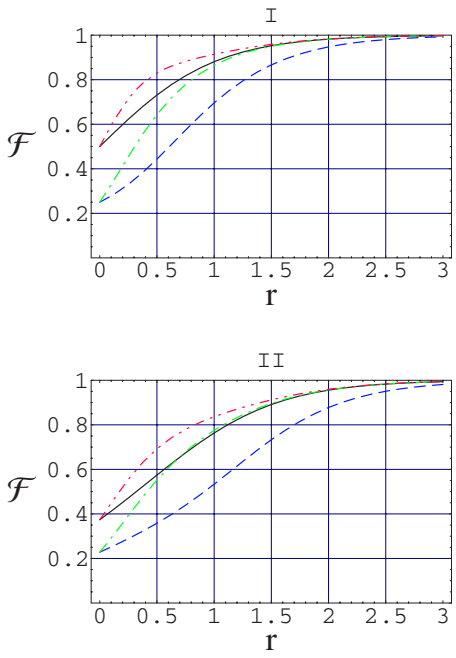

FIG. 3. (Color online) Fidelity of teleportation $\mathcal{F}$, as a function of the squeezing parameter r, with $\phi=\pi$, for input coherent states $|\beta\rangle$ (panel I) and input squeezed states $|\varepsilon\rangle$ (panel II). Comparison is given for different two-mode entangled resources: (a) Squeezed state (full line); (b) squeezed number state (dashed line); (c) photon-added squeezed state (dotted-dashed line); (d) photon-subtracted squeezed state (double-dotted, dashed line). In plot I the value of β is arbitrary. In plot II the squeezing parameter ε of the input state is fixed at modulus $s=0.8$ and phase $\varphi=0$.

Let us now consider the case of non-Gaussian input states $|1\rangle$, $(1+|\beta|^2)^{-1/2}a^\dagger|\beta\rangle$, and $S(\varepsilon)|1\rangle$, whose characteristic functions read, respectively,

$$\chi_F(\alpha_{\mathrm{in}}) = e^{-(1/2)|\alpha_{\mathrm{in}}|^2}(1-|\alpha_{\mathrm{in}}|^2), \tag{19}$$

$$\chi_{\mathrm{pac}}(\alpha_{\mathrm{in}}) = (1+|\beta|^2)^{-1}e^{-(1/2)|\alpha_{\mathrm{in}}|^2+3i\,\mathrm{Im}[\alpha_{\mathrm{in}}\beta^*]} \times(1+|\beta|^2-|\alpha_{\mathrm{in}}|^2+2i\,\mathrm{Im}[\alpha_{\mathrm{in}}\beta^*]), \tag{20}$$

$$\chi_{\mathrm{sq}F}(\alpha_{\mathrm{in}}) = e^{-(1/2)|\xi_{\mathrm{in}}|^2}(1-|\xi_{\mathrm{in}}|^2). \tag{21}$$

In Fig. 4 we plot the fidelity of teleportation for two non-Gaussian input states: The single-photon Fock state Eq. (19) (panel I), and the photon added coherent state Eq. (20) (panel II).

In panel I, we observe that both the photon-added and photon-subtracted two-mode squeezed resources (5) and (6) lead to an improvement of the fidelity with respect to the squeezed Gaussian resource. The photon-subtracted

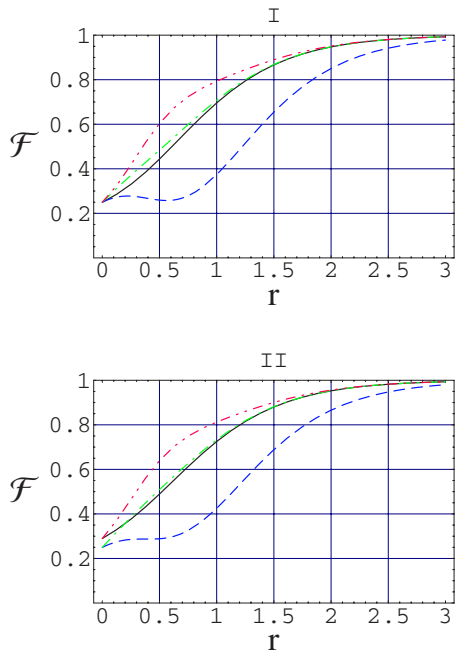

FIG. 4. (Color online) Behavior of the fidelity of teleportation $\mathcal{F}$ as a function of the squeezing parameter r, with $\phi=\pi$, for two different non-Gaussian input states: The Fock state $|1\rangle$ (panel I), and the photon-added coherent state $(1+|\beta|^2)^{-1/2}a^\dagger|\beta\rangle$ (panel II). We compare the performances obtained by using different two-mode entangled Gaussian and non-Gaussian resources: (a) Squeezed state (full line); (b) squeezed number state (dashed line); (c) photon-added squeezed state (dotted-dashed line); (d) photon-subtracted squeezed state (double-dotted-dashed line). In panel II the value of the coherent amplitude of the input photon-added coherent state is fixed at $\beta=0.3$.

squeezed state again performs better than the photon-added one, and the squeezed number state yields the poorest performance when compared to the other Gaussian and non-Gaussian resources. From panel II we see that once more the photon-subtracted resource yields the best performance at any fixed squeezing, and that the photon-added squeezed state allows for a very modest improvement in the fidelity with respect to the squeezed Gaussian reference, above a threshold value of the squeezing parameter.

In Fig. 5 we compare the fidelity of teleportation $\mathcal{F}$ for the case of a squeezed Fock input state and different Gaussian and non-Gaussian entangled resources. Comparing with panels I and II of Fig. 4, we see that the qualitative behaviors are very similar to the two previous examples of non-Gaussian input states.

From all of the above investigations, we find that the photon-subtracted squeezed state (6) is always to be preferred as entangled resource compared either to the Gaussian ones or to non-Gaussian states that are obtained by combining squeezing and photon pumping. The reason explaining this result will become clear in the next sections when we will discuss a general class of states that include as particular cases all the resources introduced so far, and that allow to single out some properties that are necessary in order to optimize the success of teleportation.

Before ending this section, it is worth remarking that the (non-Gaussian) two-mode photon-subtracted squeezed state

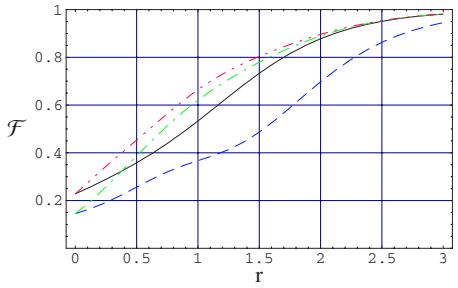

FIG. 5. (Color online) Behavior of the fidelity of teleportation $\mathcal{F}$ as a function of the squeezing parameter r, with $\phi=\pi$, for the squeezed Fock input state $S(s)|1\rangle$, using different two-mode Gaussian and non-Gaussian entangled resources: (a) Squeezed state (full line); (b) squeezed number state (dashed line); (c) photon-added squeezed state (dotted-dashed line); (d) photon-subtracted squeezed state (double-dotted-dashed line). The value of s is fixed to $s=0.8$.

can formally be defined as the first-order truncation of the (Gaussian) two-mode squeezed state. Let us first consider the twin-beam $|-2r\rangle=S_{12}(-2r)|0,0\rangle_{12}$. Such a state can be written as

$$|-2r\rangle = S_{12}(-r)S_{12}(-r)|0,0\rangle_{12} \propto S_{12}(-r)\sum_{n=0}^{\infty}\tanh^n r|n,n\rangle_{12}.$$

Therefore, truncating the series in the last expression at $n=1$, one recovers the state (6), with $\phi=\pi$, i.e., $|1^{(-)},1^{(-)};-r\rangle \propto S_{12}(-r)\{|0,0\rangle_{12}+\tanh r|1,1\rangle_{12}\}$. Moreover, expression (6) coincides with that of the photon-subtracted state introduced in Ref. [3] when one reduces to the ideal case of a beam splitter with unity transmittance.

V. TELEPORTATION WITH OPTIMIZED NON-GAUSSIAN RESOURCES

In this section we seek to optimize the fidelity of teleportation, given the Vaidman-Braunstein-Kimble protocol, by introducing a class of entangled non-Gaussian resources that include as particular cases non-Gaussian photon-added and photon-subtracted squeezed states, squeezed number states, Gaussian two-mode squeezed states, and two-mode vacua. We name these states *squeezed Bell-like states*; their general expression reads

$$|\psi\rangle_{\mathrm{SB}} = [c_1^2 + c_2^2]^{-1/2} S_{12}(\zeta)\{c_1|0,0\rangle_{12} + e^{i\theta}c_2|1,1\rangle_{12}\}, \tag{22}$$

where the c_i's are real constants. The crucial qualitative aspect of superpositions (22) lies in their intrinsic nonclassicality, even at vanishing squeezing: In the limit $r\to 0$ and for suitable choices of the parameters c_1, c_2, and θ, state (22) reduces to a proper, maximally entangled, Bell state of two qubits. On the contrary, in the limit of vanishing squeezing, the two-mode states (5) and (6) reduce to two different, factorized (disentangled) limits, respectively, the (non-Gaussian) first excited Fock state and the (Gaussian) two-mode vacuum.

States (5) and (6) can always be obtained as particular cases of state (22). For instance, fixing the choice $c_1=-1$, $c_2=\tanh r$, $\theta=\phi$, the states (22) and (6) coincide. Moreover,

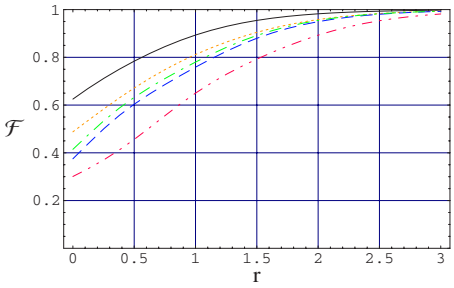

FIG. 6. (Color online) Behavior of the fidelity of teleportation $\mathcal{F}(r,\phi,\delta,\theta)$ associated to the squeezed Bell-like resource (22) with $\phi=\pi$, $\delta=\frac{\pi}{4}$, $\theta=0$, plotted as a function of the squeezing parameter r for the following input states: (a) Coherent state (full line); (b) squeezed state $|s\rangle=S(s)|0\rangle$, with $s=0.8$ (dotted line); (c) Fock state $|1\rangle$ (dashed line); (d) photon-added coherent state $(1+|\beta|^2)^{-1/2}a^\dagger|\beta\rangle$, with $\beta=0.3$ (dotted-dashed line); (e) squeezed Fock state $|s\rangle=S(s)|1\rangle$, with $s=0.8$ (double-dotted-dashed line).

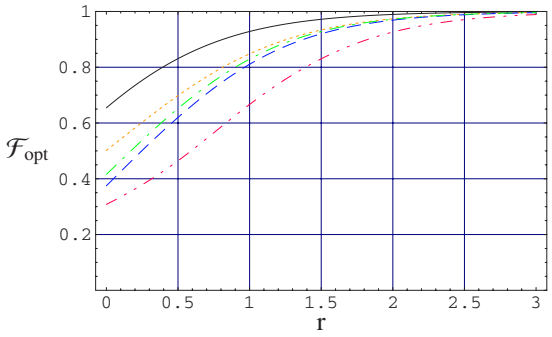

FIG. 7. (Color online) Plot of $\mathcal{F}_{\rm opt}(r)$ as a function of r for the following input states: (a) Coherent state (full line); (b) squeezed vacuum $|s\rangle=S(s)|0\rangle$, with $s=0.8$ (dotted line); (c) single-photon Fock state $|1\rangle$ (dashed line); (d) photon-added coherent state $(1+|\beta|^2)^{-1/2}a^\dagger|\beta\rangle$, with $\beta=0.3$ (dotted-dashed line); (e) squeezed Fock state $|s\rangle=S(s)|1\rangle$, with $s=0.8$ (double-dotted-dashed line).

Eq. (22) can be obtained as a superposition of Eqs. (5) and (6). A discussion of schemes for the experimental generation of states (22) is reported in Sec. VII. The characteristic function associated to the squeezed Bell-like state (22) reads

$$\chi_{\rm SB}=[c_1^2+c_2^2]^{-1}e^{-(1/2)(|\xi_1|^2+|\xi_2|^2)}\{c_1^2+2c_1c_2\,{\rm Re}[e^{i\theta}\xi_1\xi_2] + c_2^2(1-|\xi_1|^2)(1-|\xi_2|^2)\}, \tag{23}$$

where the independent variables ξ_k are defined according to Eq. (13).

Exploiting Eqs. (8) and (9), the expression for the fidelity of teleportation $\mathcal{F}$ can be determined analytically for all cases of entangled resources of the form (23) and different input states. In order to simplify notations, let us introduce the parametrization $c_1=\cos\delta$, $c_2=\sin\delta$. For each given input state, the analytic expression for the fidelity will be a function of the independent parameters r, ϕ, δ, and θ, i.e., $\mathcal{F}=\mathcal{F}(r,\phi,\delta,\theta)$. For instance, at finite squeezing and for $\delta=\frac{\pi}{4}$ and $\theta=0$, state (22) reduces to a squeezed Bell state and we may assess analytically the performance of such an entangled resource as far as teleportation is concerned. In Fig. 6 we show the behavior of the fidelity as a function of the squeezing parameter r, with $\phi=\pi$, $\delta=\frac{\pi}{4}$, $\theta=0$, for the five different input states considered in the preceding section. It is straightforward to observe that the squeezed Bell state (22) with $\delta=\frac{\pi}{4}$ and $\theta=0$, when used as entangled resource, leads to a relevant improvement of the performance, compared to all other Gaussian and non-Gaussian resources that we have investigated in the preceding section.

We do not report the explicit analytic expressions of the fidelities associated to the squeezed Bell-like resource and to each input state, because they are rather long and cumbersome. For the same reason we have not reported the explicit expressions associated to the other non-Gaussian entangled resources in the preceding section. In fact, besides not being particularly illuminating, reporting the explicit expressions is not really needed once the explicit analysis has established that all fidelities are monotonically increasing functions of the squeezing parameter r at maximally fixed phase $\phi=\pi$. Therefore, in the following we will assume $\phi=\pi$ and, moreover, $\theta=0$, because one can check that nonvanishing values of θ do not lead to any improvement of the fidelity.

Having established such a framework, we can proceed to maximize, for each different input state, the fidelity $\mathcal{F}(r,\pi,\delta,0)$ over the Bell-superposition angle δ. At fixed squeezing $r=\tilde{r}$, we define the optimized fidelity as

$$\mathcal{F}_{\rm opt}(\tilde{r})=\max_{\delta}\mathcal{F}(\tilde{r},\pi,\delta,0). \tag{24}$$

For instance, in the case of input coherent state, the maximization of $\mathcal{F}(r,\pi,\delta,0)$, at fixed r, leads to the following determination for the optimal Bell-superposition angle $\delta_{\rm max}^{(c)}$:

$$\delta_{\rm max}^{(c)}=\tfrac{1}{2}\arctan(1+e^{-2r}), \tag{25}$$

while for an input single-photon Fock state, one finds

$$\delta_{\rm max}^{(F)}=\frac{1}{2}\arctan\left(\frac{e^{-2r}(1-e^{2r}+e^{4r}+3e^{6r})}{3(e^{2r}-1)^2}\right). \tag{26}$$

Finally, in Fig. 7 we report the behavior of the optimized fidelities $\mathcal{F}_{\rm opt}(r)$ as functions of r for all the considered input states.

A relevant improvement of the fidelity is observed in all cases, even at vanishing squeezing, due to the persistent nonclassicality of the squeezed Bell-like entangled resource in the limit $r\to 0$.

In order to quantify the increase in the probability of success for teleportation, we look at the percent increase in fidelity relative to a fixed reference. We thus define the difference between the optimized fidelity $\mathcal{F}_{\rm opt}(r)$ and the reference fidelity $\mathcal{F}_{\rm ref}(r,\pi)$, and normalize this difference by $\mathcal{F}_{\rm ref}(r,\pi)$,

$$\Delta\mathcal{F}(r)=\frac{\mathcal{F}_{\rm opt}(r)-\mathcal{F}_{\rm ref}(r,\pi)}{\mathcal{F}_{\rm ref}(r,\pi)}, \tag{27}$$

where the reference fidelity is fixed to be the one associated to a given entangled resource. In Fig. 8, the relative fidelity $\Delta\mathcal{F}(r)$ is plotted as a function of r for two different choices of the reference resource. In panel I, the reference resource is the Gaussian twin beam; in panel II the reference resource is

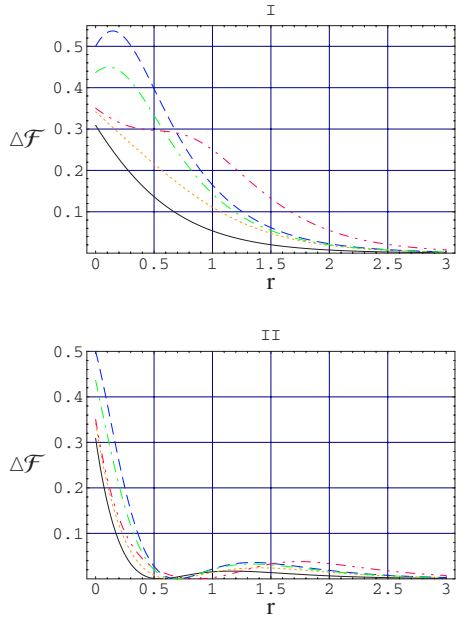

FIG. 8. (Color online) Behavior of the relative fidelity $\Delta\mathcal{F}=\mathcal{F}_{\rm opt}(r)-\mathcal{F}_{\rm ref}(r,\pi)$ as a function of r, for the following input states: (a) Coherent state (full line); (b) squeezed state $|s\rangle=S(s)|0\rangle$, with $s=0.8$ (dotted line); (c) single-photon Fock state $|1\rangle$ (dashed line); (d) photon-added coherent state $(1+|\beta|^2)^{-1/2}a^\dagger|\beta\rangle$, with $\beta=0.3$ (dotted-dashed line); (e) squeezed Fock state $|s\rangle=S(s)|1\rangle$, with $s=0.8$ (double-dotted-dashed line). In panel I the reference resource is the twin beam; in panel II the reference resource is the two-mode photon-subtracted squeezed state.

the non-Gaussian two-mode photon-subtracted squeezed state.

From panel I, as expected, we see that, at fixed squeezing (or fixed energy), the optimized non-Gaussian squeezed Bell-like resource leads to a strong percent enhancement of the teleportation fidelity (up to more than 50%) with respect to that attainable exploiting the standard Gaussian twin beam, for every value of r. Obviously, in the asymptotic limit of very large squeezing, the two resources converge to perfect teleportation efficiency. Panel II shows that use of the optimized squeezed Bell-like entangled resource (22) leads to a significant advantage with respect to exploiting the photon-subtracted squeezed state resource for low values (up to $r\simeq 0.5$) of the squeezing. Moreover, the different curves corresponding to the different input states, exhibit the same qualitative behavior. Starting from large, nonvanishing values, $\Delta\mathcal{F}(r)$ decreases monotonically and vanishes at different points in the interval $[0.5\leqslant r\leqslant 0.9]$. It then exhibits revivals with different peaks at intermediate values of the squeezing, before vanishing asymptotically for large values of r. It can be checked that for values $r=\bar{r}$ such that $\Delta\mathcal{F}(\bar{r})=0$, the squeezed Bell-like state (22) and the photon-subtracted squeezed state (6) coincide.

VI. UNDERSTANDING OPTIMIZATION: ENTANGLEMENT, NON-GAUSSIANITY, AND SQUEEZED-VACUUM AFFINITY

In this section we will investigate and determine the properties that appear to be necessary to achieve maximal teleportation success with non-Gaussian entangled resources. To this end, we analyze the entanglement and the non-Gaussianity of the squeezed Bell-like states and compare them with those of the photon-added and photon-subtracted squeezed states. In Fig. 9 we show the behavior of the von Neumann entropy $E_{\rm vN}$ for two different squeezed Bell-like resources, respectively, the one optimized for the teleportation of an input coherent state, i.e., with δ given by expression (25), and the one optimized for the teleportation of an input single-photon Fock state, i.e., with δ given by the expression (26). This behavior is compared with that of the von Neumann entropy of the photon-added and the photon-subtracted squeezed states (the two states have the same degree of entanglement at the given squeezing).

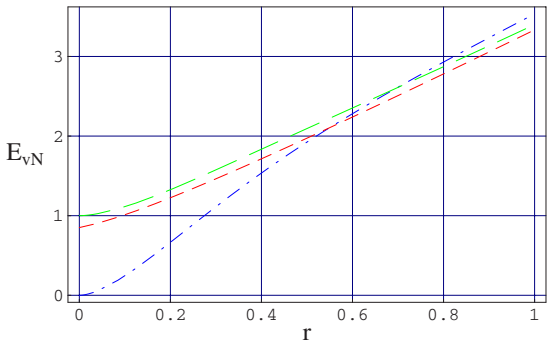

FIG. 9. (Color online) Entropy of entanglement $E_{\rm vN}$ for the squeezed Bell-like state (22), as a function of r, with δ fixed by Eqs. (25) and (26). Dashed line, $\delta=\delta^{(C)}_{\rm max}$, long dashed line, $\delta=\delta^{(F)}_{\rm max}$. The entropy of the states (5) and (6) is reported as well for comparison (dotted-dashed line).

The intersections between the curves correspond to the values $\bar{r}$ for which the squeezed Bell-like state reduces to a photon-subtracted or to a photon-added squeezed state. It is then important to observe that in the range $0<r<\bar{r}$, in which the fidelity of teleportation using optimized Bell-like resources is always maximal (see Fig. 8, panel II), the entanglement of the squeezed Bell-like state is always larger than that of the photon-subtracted (as well as photon-added) squeezed states. Therefore, a partial explanation of the better performance of squeezed Bell-like resources lies in their higher degree of entanglement compared to other non-Gaussian resources. However, from the graphs one can see that there are situations in which the entanglement of photon-added and/or photon-subtracted resources is larger but, nevertheless, the fidelity of teleportation is still below the one associated to a squeezed Bell-like resource. Entanglement is thus not the only characterizing property in order to compare the performances of different non-Gaussian resources.

From the above discussion, it is natural to look at a quantification of the non-Gaussian character of different resources, in order to compare their performances. Clearly, the subtle problem here is to define a reasonable "measure" of non-Gaussianity, endowed with some nontrivial operative meaning. Recently, inspired by the analysis of Wolf, Giedke, and Cirac on the extremality of Gaussian states [6] at fixed covariance matrix, a measure of non-Gaussianity has been introduced in terms of the Hilbert-Schmidt distance between a given non-Gaussian state and a reference Gaussian state

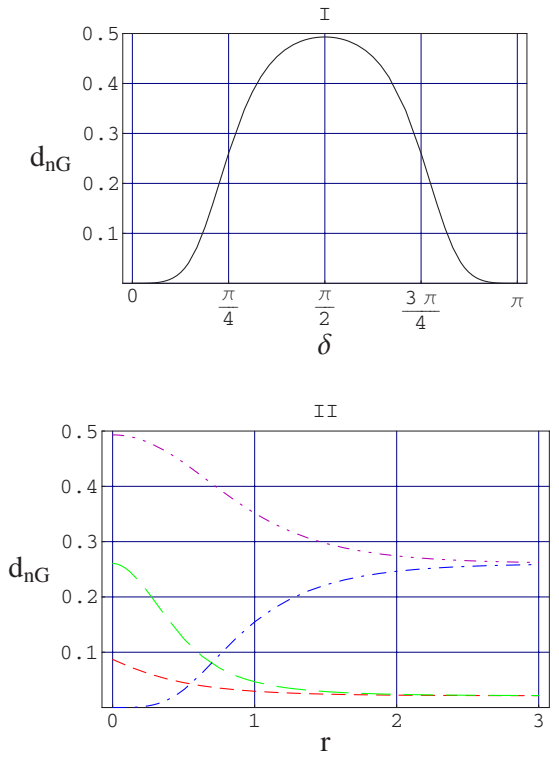

FIG. 10. (Color online) Non-Gaussianity measure d_{nG} for the squeezed Bell-like state (22). In panel I we plot d_{nG} for the state (22) as a function of δ, and for arbitrary r. Panel II reports d_{nG} for the state (22) as a function of r and for δ fixed at the optimized values $\delta=\delta_{\max}^{(C)}$ (dashed line), and $\delta=\delta_{\max}^{(F)}$ (long dashed line), see Eqs. (25) and (26). For comparison the measures for the states (5) (double-dotted-dashed line) and (6) (dotted-dashed line) are also reported.

with the same covariance matrix [36]. Given a generic state ρ, its non-Gaussian character can be quantified through the distance d_{nG} between ρ and the reference Gaussian state ρ_{G}, defined according to the following relation:

$$d_{\mathrm{nG}}=\frac{\mathrm{Tr}[(\rho-\rho_{\mathrm{G}})^2]}{2\,\mathrm{Tr}[\rho^2]}=\frac{\mathrm{Tr}[\rho^2]+\mathrm{Tr}[\rho_{\mathrm{G}}^2]-2\,\mathrm{Tr}[\rho\rho_{\mathrm{G}}]}{2\,\mathrm{Tr}[\rho^2]}, \tag{28}$$

where, as already mentioned, the Gaussian state ρ_{G} is completely determined by fixing for it the same covariance matrix and the same first-order mean values of the quadrature operators associated to state ρ. Using this definition, in Fig. 10 we report the behavior of the *non Gaussianity* d_{nG} for the squeezed Bell-like state (22).

The quantity d_{nG} depends only on the parameter δ (see panel I), as the non-Gaussianity of the state cannot change under symplectic squeezing operations. For δ in the interval $[0,\pi]$, d_{nG} attains its maximum at $\delta=\frac{\pi}{2}$: At that point, the Bell-like state reduces to a Fock state. In fact, as expected, a (squeezed) number state must be more strongly non-Gaussian than a (squeezed) superposition of the vacuum and of a Fock state. In panel II, we report the behavior of d_{nG} for the squeezed Bell-like resources optimized for the teleportation of a coherent state input and a single-photon Fock state input, i.e., respectively, with $\delta=\delta_{\max}^{(C)}$, and $\delta=\delta_{\max}^{(F)}$. For comparison, we plot as well the non-Gaussianity d_{nG} for the photon-added and the photon-subtracted squeezed states. The intersection points occur once again at the points $\bar{r}$ where the squeezed Bell-like states reduce to the photon-subtracted squeezed states. For r in the range $[0,\bar{r}]$, the optimized squeezed Bell-like resources are not only highly more entangled but as well strongly more non-Gaussian than the photon-subtracted squeezed states. One should note that $\lim_{r\to+\infty}\delta_{\max}^{(C)}=\lim_{r\to+\infty}\delta_{\max}^{(F)}=1$. Therefore, for very large squeezing the two optimized squeezed Bell-like resources tend to the state $S_{12}(-r)\{\cos\frac{\pi}{8}|0,0\rangle_{12}+\sin\frac{\pi}{8}|1,1\rangle_{12}\}$, which exhibits a dominating Gaussian component. On the other hand, for large r, the squeezed photon-added and photon-subtracted squeezed states asymptotically tend to a squeezed Bell state (corresponding to $\delta_{\max}=\frac{\pi}{4}$), which has balanced Gaussian and non-Gaussian contributions.

We have compared the non-Gaussianity of the different resources according to a measure that is reference dependent. One might think to define the measure according to an absolute reference. Observing that the squeezed Bell-like states and the photon-added and/or photon-subtracted squeezed states are all obtained through a degaussification protocol from a pure squeezed state, one could modify the definition (28) by taking the twin-beam $|\zeta'\rangle_{12}$ ($\zeta'=r'e^{i\phi'}$) as the universal reference Gaussian state ρ_{G}. Adopting this modified definition, and observing that the non-Gaussian states are to be compared and the reference Gaussian states are all pure, Eq. (28) reduces to $d_{\mathrm{nG}}=\min_{r',\phi'}\{1-\mathrm{Tr}[\rho\rho_{\mathrm{G}}]\}$, where the minimization is constrained to run over the squeezing parameters ζ' of the reference twin beam. However, it turns out that this modified definition provides results and information qualitatively analogous to those obtained by applying the original definition.

There is still one property that plays a crucial role in the sculpturing of an optimized CV non-Gaussian entangled resource. From Figs. 9 and 10 we see that at sufficiently large squeezing the photon-added and photon-subtracted squeezed resources have entanglement comparable to that of the optimized squeezed Bell-like states and, moreover, possess stronger non-Gaussianity. Yet, even in this regime, they are not able to perform better than the optimized Bell-like resources. This fact can be understood as follows, leading to the definition of the *squeezed-vacuum affinity*: It is well known that the Gaussian twin beam in the limit of infinite squeezing realizes exactly the CV version of the maximally entangled Bell state in the case of qubits. These two ideal resources, respectively, in the CV and qubit case, allow perfect quantum teleportation with maximal, unit fidelity. Therefore, we argue that, even when exhibiting enhanced properties of non-Gaussianity and entanglement, any efficient resource for CV quantum information tasks should enjoy a further property, i.e., to resemble the form of a two-mode squeezed vacuum, as much as possible, in the large r limit.

The *squeezed-vacuum affinity* can be quantified by the following maximized overlap:

$$\mathcal{G}=\max_{s}|_{12}\langle -s|\psi_{\mathrm{res}}(r)\rangle_{12}|^2, \tag{29}$$

where $|-s\rangle_{12}$ is a two-mode squeezed vacuum with real squeezing parameter $-s$, and $|\psi_{\mathrm{res}}(r)\rangle_{12}$ is any entangled two-

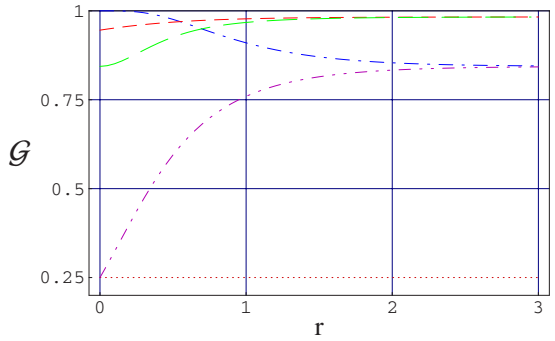

FIG. 11. (Color online) Maximized overlap $\mathcal{G}$ between a twin beam and different non-Gaussian entangled resources $|\psi_{\rm res}(r)\rangle_{12}$ as a function of r. Dashed line, squeezed Bell-like state with δ fixed at the optimized value $\delta=\delta_{\rm max}^{(C)}$. Long dashed line, the same with δ fixed at the optimized value $\delta=\delta_{\rm max}^{(F)}$. For comparison, we plot as well the maximized overlap with the photon-added squeezed state (5) (double-dotted-dashed line); the photon-subtracted squeezed state (6) (doted-dashed line); and the single-photon squeezed number state (4) (dotted line).

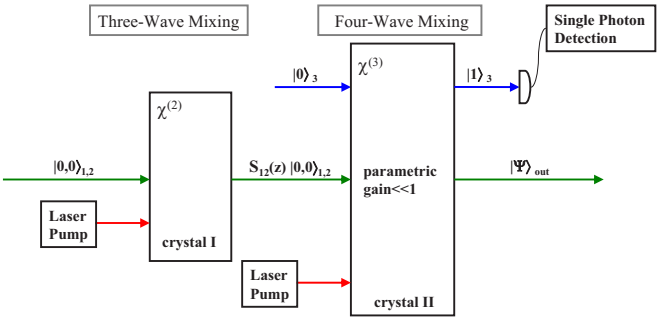

FIG. 12. (Color online) Scheme for the generation of the photon-added squeezed state (5) and of the photon-subtracted squeezed state (6). Two nonlinear crystals are used in a cascaded configuration. The first $\chi^{(2)}$ crystal is part of a three-wave mixer, acting as a parametric amplifier for the production of a two-mode squeezed state $|\zeta\rangle$. The squeezed state seeds the successive nonlinear process, a four-wave mixing interaction occurring in a $\chi^{(3)}$ crystal. A final conditional measurement reduces the multiphoton state to a photon-added and/or photon-subtracted squeezed state $|\Psi\rangle_{\rm out}$.

mode resource that depends uniquely on the squeezing r as the only free parameter. This definition applies straightforwardly to the photon-added and photon-subtracted squeezed resources, and as well to the squeezed Bell-like resources after optimization with respect to the input state. The maximization over s is imposed in order to determine, at fixed r, the twin beam that is most affine to the non-Gaussian resource being considered.

In Fig. 11 we study the behavior of the overlap $\mathcal{G}$ as a function of the squeezing r for different non-Gaussian entangled resources.

From Fig. 11 one observes that maximal affinity, and close to unity, is always and beautifully achieved, at large values of the squeezing parameter, by the optimized squeezed Bell-like resources, while the lowest, constant affinity is always exhibited by the squeezed number states.

In conclusion, optimized squeezed Bell-like resources are the ones that in all squeezing regimes are closest to the simultaneous maximization of entanglement, non-Gaussianity, and affinity to the two-mode squeezed vacuum. The optimized interplay of these three properties explains the ability of squeezed Bell-like states to yield better performances, when used as resources for CV quantum teleportation, in comparison both to Gaussian resources at finite squeezing and to the standard degaussified resources such as the photon-added and the photon-subtracted squeezed states. In the next section we will discuss methods and schemes for the experimental production of squeezed Bell-like entangled resources.

VII. METHODS FOR THE GENERATION OF DEGAUSSIFIED AND SQUEEZED BELL-LIKE RESOURCES

While two-mode (Gaussian) squeezed states are currently produced in the laboratory, the experimental generation of non-Gaussian (nonclassical) states in quantum optics is still a hard task, as it requires the availability of large nonlinearities and/or the arrangement of proper apparatus for conditional measurements. Nevertheless, some truly remarkable realizations of single-mode non-Gaussian states have been recently carried out through the use of parametric amplification plus post-selection [12–14]. Recently, by a generalization of the experimental setup used in Ref. [14] to a two-mode configuration, Kitagawa *et al.* proposed a method for the generation of a certain class of two-mode photon-subtracted states [3].

Here, in some analogy with Ref. [12], we propose a possible experimental setup for the generation of the states (5) and (6), and of the squeezed Bell-like states (22). The scheme, based on a configuration of cascaded crystals, is depicted in Fig. 12.

In the first stage, by means of a three-wave mixer, functioning as a parametric amplifier, a two-mode squeezed state $|\zeta\rangle=S_{12}(\zeta)|0,0\rangle_{12}$ is produced. In the second stage, a four-wave mixing process takes place in a crystal with third order nonlinear susceptibility $\chi^{(3)}$. We consider two possible multiphoton interactions, in the travelling wave configuration, described by the following Hamiltonians:

$$H_I^{(A)}=\kappa_A a_1^\dagger a_2^\dagger a_3^\dagger+\kappa_A^* a_1 a_2 a_3, \tag{30}$$

$$H_I^{(B)}=\kappa_B a_1 a_2 a_3^\dagger+\kappa_B^* a_1^\dagger a_2^\dagger a_3, \tag{31}$$

where a_i $(i=1,2,3)$ denotes three quantized modes of the radiation field. The complex parameters κ_A and κ_B are proportional to the third-order nonlinearity and to the amplitude of an intense coherent pump field, treated classically in the regime of parametric approximation. The two-mode squeezed state seeds modes 1 and mode 3 is initially in the vacuum state $|0\rangle_3$; mode 4 is the classical pump. Energy conservation and phase matching are assumed throughout. Let us remark that, due to the typical orders of magnitudes of the third-order susceptibilities, the parametric gains are very small $|\kappa_A|$, $|\kappa_B|\ll 1$. The propagation (time evolution) in the crystal yields $|\Psi_I^{(L)}\rangle=\exp\{-itH_I^{(L)}\}|\zeta\rangle_{12}|0\rangle_3$ $(L=A,B)$. Trun-

cating the series expansion of the evolution operator at the first order in $\tilde{\kappa}_L = -it\kappa_L$, we get

$$|\Psi_I^{(A)}\rangle \approx \{1 + \tilde{\kappa}_A a_1^\dagger a_2^\dagger a_3^\dagger\}|\zeta\rangle_{12}|0\rangle_3, \tag{32}$$

$$|\Psi_I^{(B)}\rangle \approx \{1 + \tilde{\kappa}_B a_1 a_2 a_3^\dagger\}|\zeta\rangle_{12}|0\rangle_3. \tag{33}$$

Finally, a conditional measurement is performed on mode 3, consisting in a single-photon detection, i.e., a projection onto the state $|1\rangle_3$. The post-selection reduces the states (32) and (33), respectively, to the states (5) and (6). It is worth noting that the low values of the parametric gains do not affect the implementation of the process. In fact, it is analogous to require low reflectivity of a beam splitter to generate photon addition and/or photon subtraction by using linear optics.

Regarding the production of the squeezed number state (4), it can be generated, in principle, by seeding a parametric amplifier with single-photon states in the two modes.

Let us now turn to the experimental generation of the squeezed Bell-like states (22). They can be engineered by using the same setup illustrated in Fig. 12, and by simultaneously realizing inside the nonlinear crystal the processes corresponding to the interactions (30) and (31). In this case the fundamental requirements are that of energy conservation and phase matching for each multiphoton interaction must hold simultaneously at each stage. This condition can be satisfied by suitably exploiting the phenomenon of birefringence in a negative uniaxial crystal [37]. In particular, the following set of equations must hold:

$$\Omega_1 = \omega_1 + \omega_2 + \omega_3,$$

$$K_1^{\text{ext}} = k_1^{\text{ord}} + k_2^{\text{ord}} + k_3^{\text{ext}}, \tag{34}$$

$$\Omega_2 + \omega_1 + \omega_2 = \omega_3,$$

$$K_2^{\text{ord}} + k_1^{\text{ord}} + k_2^{\text{ord}} = k_3^{\text{ext}}, \tag{35}$$

where ω_j and k_j^λ $(j=1,2,3)$ represent the frequencies and the wave vectors of the quantized modes with polarization λ; Ω_j and K_j^λ $(j=1,2)$ represent the frequencies and the wave vectors of the classical pump fields; the superscript ord and ext denote, respectively, the ordinary and extraordinary polarizations for the propagating waves. A collinear configuration is assumed for the geometry of propagation inside the crystal. Then, at fixed ω_1 and ω_2, the energy conservation relations, the type-II phase matching condition in Eq. (34), and the type-I phase matching condition in Eq. (35) can be, in principle, satisfied by a suitable choice of ω_3, Ω_1, Ω_2, and of the phase-matching angle between the direction of propagation and the optical axis. Various examples of such simultaneous multiphoton processes have been demonstrated both theoretically and experimentally [1,38–42]. The final conditional measurement on mode 3 yields the superposition state

$$|\Psi_I\rangle \approx \tilde{\kappa}_A a_1^\dagger a_2^\dagger S_{12}(\zeta)|0,0\rangle_{12} + \tilde{\kappa}_B a_1 a_2 S_{12}(\zeta)|0,0\rangle_{12}. \tag{36}$$

By applying a standard Bogoliubov transformation and after a little algebra, it is straightforward to show that superposition state (36) reduces to the squeezed Bell-like state (22) if

$$c_1 = -(e^{-i\phi}\tilde{\kappa}_A \tanh r + e^{i\phi}\tilde{\kappa}_B),$$

$$c_2 = \tilde{\kappa}_A + e^{2i\phi}\tilde{\kappa}_B \tanh r. \tag{37}$$

The latter conditions can be successfully implemented by observing that the complex parameters $\tilde{\kappa}_A$ and $\tilde{\kappa}_B$ can be controlled to a very high degree by means of the amplitudes of the external classical pumps.

VIII. CONCLUSIONS AND OUTLOOK

In this work we have presented a thorough comparison, with regard to the performance in continuous-variable quantum teleportation, between standard degaussified resources such as photon-added and photon-subtracted squeezed states and a type of *sculptured* resource that interpolates between different degaussified states and can be optimized because it depends on an extra, relative-phase, independent free parameter in addition to squeezing. These sculptured non-Gaussian resources are what we have named *squeezed Bell-like states*: They hybridize discrete single-photon pumping, coherent superposition of Bell two-qubit eigenstates, and continuous-variable squeezing. The maximization of the teleportation fidelity with respect to different inputs, including coherent and squeezed states, is achieved by squeezed Bell-like states in comparison both to Gaussian and other non-Gaussian resources, and for all values of squeezing, including the asymptotic Einstein-Podolsky-Rosen limit. Understanding this enhancement yielded by the squeezed Bell-like resources in the teleportation success is possible when interpreted in terms of a multiple optimization problem. The squeezed Bell-like states are those states that are as close as possible to the simultaneous maximization of entanglement, non-Gaussianity, and affinity to the two-mode squeezed vacuum. The analysis performed in the case of pure-state resources can be extended to the case of mixed-state resources in the presence of noise, imperfections, and other sources of decoherence: We plan to report the results on the study of these situations in the near future.

The concepts of hybridization, sculpturing, and optimization suggest that the present investigation could be extended and generalized along several directions. Further optimization is in principle possible with respect to the local parts of the resource states, in analogy to the case of standard Gaussian resources [43]. One could think of extending the sculpturing to the entire basis of Bell states, to generate entangled non-Gaussian resources that can never be reduced to proper truncations of Gaussian squeezed resources. Such "fully sculptured" resources might allow for the further enhancement of the teleportation success due to the presence of a larger number of experimentally adjustable free parameters in addition to squeezing. Fully sculptured states could be applied to hybrid schemes of teleportation combining continuous-variable inputs with discrete-variable resources and vice versa. In this framework, a particularly appealing line of research would be to look for modified schemes of teleportation beyond the standard Braunstein-Kimble protocol, to be realized by generalized measurements in combination with state-control enhancing unitary operations. Finally,

the present discussion could be extended to other types of quantum information tasks and processes besides teleportation. For instance, it would be interesting to investigate the comparative effects of non-Gaussian inputs and non-Gaussian resources in schemes for the generation of macroscopic and mesoscopic optomechanical entanglement [44].

ACKNOWLEDGMENTS

The authors acknowledge financial support from MIUR, under PRIN National Research Program 2005, from CNR-INFM Coherentia, from CNISM, from INFN, under the special HALODYST program, and from ISI Foundation for Scientific Interchange.

[1] See, for instance, F. Dell'Anno, S. De Siena, and F. Illuminati, Phys. Rep. **428**, 53 (2006), and references therein.
[2] M. S. Kim, W. Son, V. Bužek, and P. L. Knight, Phys. Rev. A **65**, 032323 (2002).
[3] A. Kitagawa, M. Takeoka, M. Sasaki, and A. Chefles, Phys. Rev. A **73**, 042310 (2006).
[4] V. V. Dodonov and L. A. de Souza, J. Opt. B: Quantum Semiclassical Opt. **7**, S490 (2005).
[5] A. P. Lund, T. C. Ralph, and P. van Loock, e-print arXiv:quant-ph/0605247 (to be published).
[6] M. M. Wolf, G. Giedke, and J. I. Cirac, Phys. Rev. Lett. **96**, 080502 (2006).
[7] G. S. Agarwal and K. Tara, Phys. Rev. A **43**, 492 (1991).
[8] G. Bjork and Y. Yamamoto, Phys. Rev. A **37**, 4229 (1988).
[9] Z. Zhang and H. Fan, Phys. Lett. A **165**, 14 (1992).
[10] M. Dakna, T. Anhut, T. Opatrný, L. Knöll, and D.-G. Welsch, Phys. Rev. A **55**, 3184 (1997).
[11] M. S. Kim, E. Park, P. L. Knight, and H. Jeong, Phys. Rev. A **71**, 043805 (2005).
[12] A. Zavatta, S. Viciani, and M. Bellini, Science **306**, 660 (2004).
[13] A. I. Lvovsky and S. A. Babichev, Phys. Rev. A **66**, 011801(R) (2002).
[14] J. Wenger, R. Tualle-Brouri, and P. Grangier, Phys. Rev. Lett. **92**, 153601 (2004).
[15] S. Lloyd and S. L. Braunstein, Phys. Rev. Lett. **82**, 1784 (1999).
[16] S. L. Braunstein and H. J. Kimble, Phys. Rev. Lett. **80**, 869 (1998).
[17] A. Furusawa, J. L. Sørensen, S. L. Braunstein, C. A. Fuchs, H. J. Kimble, and E. S. Polzik, Science **282**, 706 (1998).
[18] W. P. Bowen, N. Treps, B. C. Buchler, R. Schnabel, T. C. Ralph, Hans-A. Bachor, T. Symul, and P. K. Lam, Phys. Rev. A **67**, 032302 (2003).
[19] N. Takei, H. Yonezawa, T. Aoki, and A. Furusawa, Phys. Rev. Lett. **94**, 220502 (2005).
[20] S. L. Braunstein and P. van Loock, Rev. Mod. Phys. **77**, 513 (2005).
[21] T. Opatrný, G. Kurizki, and D.-G. Welsch, Phys. Rev. A **61**, 032302 (2000).
[22] P. T. Cochrane, T. C. Ralph, and G. J. Milburn, Phys. Rev. A **65**, 062306 (2002).
[23] S. Olivares, M. G. A. Paris, and R. Bonifacio, Phys. Rev. A **67**, 032314 (2003).
[24] N. J. Cerf, O. Krüger, P. Navez, R. F. Werner, and M. M. Wolf, Phys. Rev. Lett. **95**, 070501 (2005).
[25] P. van Loock, W. J. Munro, K. Nemoto, T. P. Spiller, T. D. Ladd, S. L. Braunstein, and G. J. Milburn, e-print arXiv:quant-ph/0701057.
[26] T. C. Ralph, A. Gilchrist, G. J. Milburn, W. J. Munro, and S. Glancy, Phys. Rev. A **68**, 042319 (2003).
[27] T. P. Spiller, K. Nemoto, S. L. Braunstein, W. J. Munro, P. van Loock, and G. J. Milburn, New J. Phys. **8**, 30 (2006).
[28] C. H. Bennett, G. Brassard, C. Crepeau, R. Jozsa, A. Peres, and W. K. Wootters, Phys. Rev. Lett. **70**, 1895 (1993).
[29] D. Bouwmeester, J. W. Pan, K. Mattle, M. Eibl, H. Weinfurter, and A. Zeilinger, Nature (London) **390**, 575 (1997).
[30] D. Boschi, S. Branca, F. De Martini, L. Hardy, and S. Popescu, Phys. Rev. Lett. **80**, 1121 (1998).
[31] L. Vaidman, Phys. Rev. A **49**, 1473 (1994).
[32] S. J. van Enk, Phys. Rev. A **60**, 5095 (1999).
[33] A. Vukics, J. Janszky, and T. Kobayashi, Phys. Rev. A **66**, 023809 (2000).
[34] H. F. Hofmann, T. Ide, T. Kobayashi, and A. Furusawa, Phys. Rev. A **62**, 062304 (2000).
[35] P. Marian and T. A. Marian, Phys. Rev. A **74**, 042306 (2006).
[36] M. G. Genoni, M. G. A. Paris, and K. Banaszek, e-print arXiv:0704.0639v2 (to be published).
[37] J. E. Midwinter and J. Warner, Br. J. Appl. Phys. **16**, 1667 (1965).
[38] R. A. Andrews, H. Rabin, and C. L. Tang, Phys. Rev. Lett. **25**, 605 (1970).
[39] M. E. Smithers and E. Y. C. Lu, Phys. Rev. A **10**, 1874 (1974).
[40] A. Ferraro, M. G. A. Paris, M. Bondani, A. Allevi, E. Puddu, and A. Andreoni, J. Opt. Soc. Am. B **21**, 1241 (2004); M. Bondani, A. Allevi, A. Andreoni, E. Puddu, A. Ferraro, and M. G. A. Paris, Opt. Lett. **29**, 180 (2004).
[41] O. Pfister, S. Feng, G. Jennings, R. Pooser, and D. Xie, Phys. Rev. A **70**, 020302(R) (2004); R. C. Pooser and O. Pfister, Opt. Lett. **30**, 2635 (2005).
[42] M. K. Olsen and A. S. Bradley, Phys. Rev. A **74**, 063809 (2006).
[43] G. Adesso and F. Illuminati, Phys. Rev. Lett. **95**, 150503 (2005).
[44] D. Vitali, S. Gigan, A. Ferreira, H. R. Böhm, P. Tombesi, A. Guerreiro, V. Vedral, A. Zeilinger, and M. Aspelmeyer, Phys. Rev. Lett. **98**, 030405 (2007); S. Bose, K. Jacobs, and P. L. Knight, Phys. Rev. A **56**, 4175 (1997).